

# Group Communication with Context Codec for Ultra-Lightweight Source Separation

Yi Luo, Cong Han, Nima Mesgarani

**Abstract**—Ultra-lightweight model design is an important topic for the deployment of existing speech enhancement and source separation techniques on low-resource platforms. Various lightweight model design paradigms have been proposed in recent years; however, most models still suffer from finding a balance between model size, model complexity, and model performance. In this paper, we propose the group communication with context codec (GC3) design to decrease both model size and complexity without sacrificing the model performance. Group communication splits a high-dimensional feature into groups of low-dimensional features and applies a module to capture the inter-group dependency. A model can then be applied to the groups in parallel with a significantly smaller width. A context codec is applied to decrease the length of a sequential feature, where a context encoder compresses the temporal context of local features into a single feature representing the global characteristics of the context, and a context decoder decompresses the transformed global features back to the context features. Experimental results show that GC3 can achieve on par or better performance than a wide range of baseline architectures with as small as 2.5% model size.

**Keywords**—*Source separation, deep learning, lightweight, group communication, context codec*

## I. INTRODUCTION

Recent developments in the neural network architectures have significantly advanced the state-of-the-art source separation problem. While researchers have shown that large neural networks can achieve superb performance on various machine learning problems, one important topic for network design, especially for the source separation problem, is to constrain the model size and complexity so that such models can be properly deployed to low-resource platforms such as mobile and wearable devices.

Tremendous efforts have been made to propose novel model architectures and model compression techniques. Early deep neural networks used for source separation contained stacked recurrent layers such as LSTM layers with a relatively large number of hidden units [1]–[5], and the corresponding model sizes were typically over tens of millions of parameters with high model complexity. Convolutional neural networks (CNNs) have also been explored in both time-frequency domain [6]–[11] and time domain [12]–[18], and researchers have begun to focus on decreasing the model size and complexity while maintaining or improving the performance. Moreover, the combination of recurrent and convolutional layers has also been a popular topic for real-time model design, and various convolutional recurrent networks have been proposed [19]–[24]. Better layer organization within the network have also been investigated [25]–[29], which further decrease the

overall model size and maintain the separation fidelity. Beyond directly designing smaller models, neural architecture search (NAS) techniques have also been utilized to automatically search for compact architectures for speech-related tasks [30], [31], teacher-student learning methods have been explored for obtaining low-latency separation models [32], quantization and binarization algorithms have been studied for low-resource separation systems [33]–[35], and network pruning and distillation strategies can further be applied to decrease the model size [36], [37]. However, compared with directly designing lightweight architectures, existing model compression or quantization techniques typically introduce different levels of degradation on the model performance, and the tradeoff between the complexity and performance drop needs to be carefully considered. Thus, finding smaller and better architectures is still preferred.

A recent study introduced *group communication* (*GroupComm*) [38], a module motivated by subband and multiband processing models such as frequency-LSTM (F-LSTM) [39]–[42], which can easily change a model into an ultra-lightweight counterpart. GroupComm splits a high-dimensional feature, such as a spectrum, into groups of low-dimensional features, such as subband spectra, and uses the same model across all the groups for weight sharing. Another inter-group module is applied to capture the dependencies within the groups, so that the processing of each group always depends on the global information available. Compared with conventional F-LSTM or other similar architectures that explicitly model time and frequency dependencies where the subband features are concatenated back to the fullband feature [43]–[45], GroupComm does not perform such concatenation but simply applies a small module to communicate across the groups. Moreover, the low-dimensional features enable the use of a smaller module, e.g., CNN or RNN layer, than the original high-dimensional feature, and together with weight sharing the total model size can be significantly reduced. Experimental results showed that the GroupComm-equipped model can achieve on par performance with the baseline model in the noisy reverberant speech separation task with a 2.8% model size and 43.5% multiply-accumulate (MAC) operations [46], a common metric for evaluating model complexity.

It is worth noting that although GroupComm can drastically decrease the model size, model complexity is still relatively high. Moreover, memory consumption in the GroupComm-equipped models is much higher than that in the baseline models, which may not only pose constraints on its applications but also significantly increase the training cost. In this paper, we introduce a *context codec* module to help GroupComm maintain the performance while further decreasing the number

of MAC operations, accelerating the training speed and alleviating the memory consumption in both training and inference time. A context codec module contains a context encoder and a context decoder, where the context encoder summarizes the temporal context of local features into a single feature representing the global characteristics of the context, and a context decoding module transforms the compressed feature back to the context features. Squeezing the input contexts into higher-level representations corresponds to a nonlinear downsampling step that can significantly decrease the length of a feature sequence. Note that compared with other architectures that perform iterative downsampling and upsampling steps [12], [18], the context codec is only applied once and all remaining modeling steps are applied on the downsampled features, which enables a smaller memory footprint and faster training speed. We call the combination of **GroupComm** and **Context Codec** the **GC3** design.

The original GroupComm module applied a bidirectional LSTM (BLSTM) layer for inter-group processing. In this paper, we also explore different network architectures for the GroupComm module and investigate the effect of different hyperparameters in the system configuration. Experimental results show that by applying GC3 in a dual-path RNN (DPRNN) baseline [25], the GC3-DPRNN can achieve on par performance with the baseline DPRNN with 4.7% model size and 17.6% MAC operations. Moreover, GC3-DPRNN only suffers from a 4% relative performance degradation compared with the baseline DPRNN with a 2.2% model size and 11.8% MAC operations. In addition to DPRNN, we also apply GC3 to two other CNN-based architectures and one transformer-based architecture and show that the GC3-equipped CNN model can significantly improve the overall performance with as few as 2.5% model size and 33.7% MAC operations, and the GC3-equipped transformer model can maintain on par performance with 4.6% model size and 17.7% MAC operations. These results prove that GC3 is a universal plug-and-play module suitable for a wide range of architectures.

The rest of the paper is organized as follows. Section II introduces the GC3 design and discusses the applicable model architectures. Section III provides the experiment configurations. Section IV analyzes the experimental results. Section V concludes the paper.

## II. GROUP COMMUNICATION WITH CONTEXT CODEC

### A. Group Communication

Given a high-dimensional feature vector  $\mathbf{h} \in \mathbb{R}^N$ ,  $\mathbf{h}$  can be decomposed into  $K$  groups of low-dimensional feature vectors  $\{\mathbf{g}^i\}_{i=1}^K$  with  $\mathbf{g}^i \in \mathbb{R}^M$ . When there is no overlap between the groups, we have  $N = KM$ . A group communication (GroupComm) module is applied across the group of vectors to capture the inter-group dependencies:

$$\{\hat{\mathbf{g}}^i\}_{i=1}^K = \mathcal{F}(\{\mathbf{g}^i\}_{i=1}^K) \quad (1)$$

where  $\hat{\mathbf{g}}^i \in \mathbb{R}^P$  is the transformed feature vector for group  $i$ , and  $\mathcal{F}(\cdot)$  is the mapping function defined by the module. Instead of concatenating  $\{\hat{\mathbf{g}}^i\}_{i=1}^K$  back to a high-dimensional feature vector and using a large module for the processing

at the next step, all  $\hat{\mathbf{g}}^i$  are passed to a shared small module to save the model size and complexity. For a sequence of features  $\mathbf{H} \in \mathbb{R}^{N \times T}$ , we assume that GroupComm is applied independently at each time step. Figure 1 (B) presents the flowchart for the GroupComm-based pipeline. For a deep architecture for sequential modeling, a GroupComm module is added before each group-shared sequence modeling module [38].

### B. GroupComm with Context Codec

In time-domain models such as the time-domain audio separation network (TasNet) where a 1-D convolutional waveform encoder is applied to replace the complex-valued short-time Fourier transform (STFT) [14], [47], the length and number of the convolution kernels in the encoder play an important role in the overall performance. It has been studied that shorter kernel length can lead to a better separation performance, and a higher overcompleteness ratio on the number of kernels can also result in a better model [14]. Such observation makes the use of long 1-D convolution kernels less straightforward, as it may require very high-dimensional encoder outputs (i.e., large  $N$ ) and further require the width of the separation module to be large to properly model them. However, shorter kernels lead to longer sequences (i.e. large  $T$ ) and higher model complexity. How to decrease the sequence length while maintaining the model performance is thus an important question in such models.

A *Context codec* is proposed here to compress the context of feature vectors into a single summarization vector as a nonlinear downsampling step and decompress the vector back to a context as a nonlinear upsampling step. A context codec contains a context encoding module and a context decoding module. Given the sequence of features  $\mathbf{H}$ , the context encoder splits  $\mathbf{H}$  along the temporal dimension into blocks  $\{\mathbf{D}^i\}_{i=1}^R \in \mathbb{R}^{N \times C}$ , where  $C$  denotes the context size and  $R$  denotes the number of context blocks. Each  $\mathbf{D}^i$  is then encoded into a single vector  $\mathbf{p}^i \in \mathbb{R}^W$  by the context encoder, resulting in a sequence of summarization vectors  $\mathbf{P} \triangleq \{\mathbf{p}^i\}_{i=1}^R \in \mathbb{R}^{W \times R}$  with  $R \ll T$ . Any processing modules can then be applied on  $\mathbf{P}$  instead of  $\mathbf{H}$  to perform temporal dependency modeling. The transformed feature are denoted as  $\hat{\mathbf{P}} \in \mathbb{R}^{W \times R}$ , and a context decoding module adds  $\hat{\mathbf{p}}^i$  to each time step in  $\mathbf{D}^i$  and applies a nonlinear transformation to generate  $\hat{\mathbf{D}}^i \in \mathbb{R}^{N \times C}$  for context  $i$ . Overlap-add is then applied on  $\{\hat{\mathbf{D}}^i\}_{i=1}^R$  to form the sequence of features  $\hat{\mathbf{H}} \in \mathbb{R}^{N \times T}$  of the original length.

For configurations where a 50% overlap is applied between context blocks, we have  $R = 2T/C$ . In network architectures where a deep module is applied for the sequence modeling part, the computational cost is  $C/2$  times smaller than using the original sequence features for modeling. To save overall model complexity, we only need to adjust  $C$  to balance performance and complexity, and properly design the model architecture for the context codec so that the computational cost for encoding and decoding introduced to the entire system is not too large. Applying GroupComm to the context codec modules can achieve this goal, and we refer to such a combination as the GC3 design. Figure 1 (C) provides the flowchart

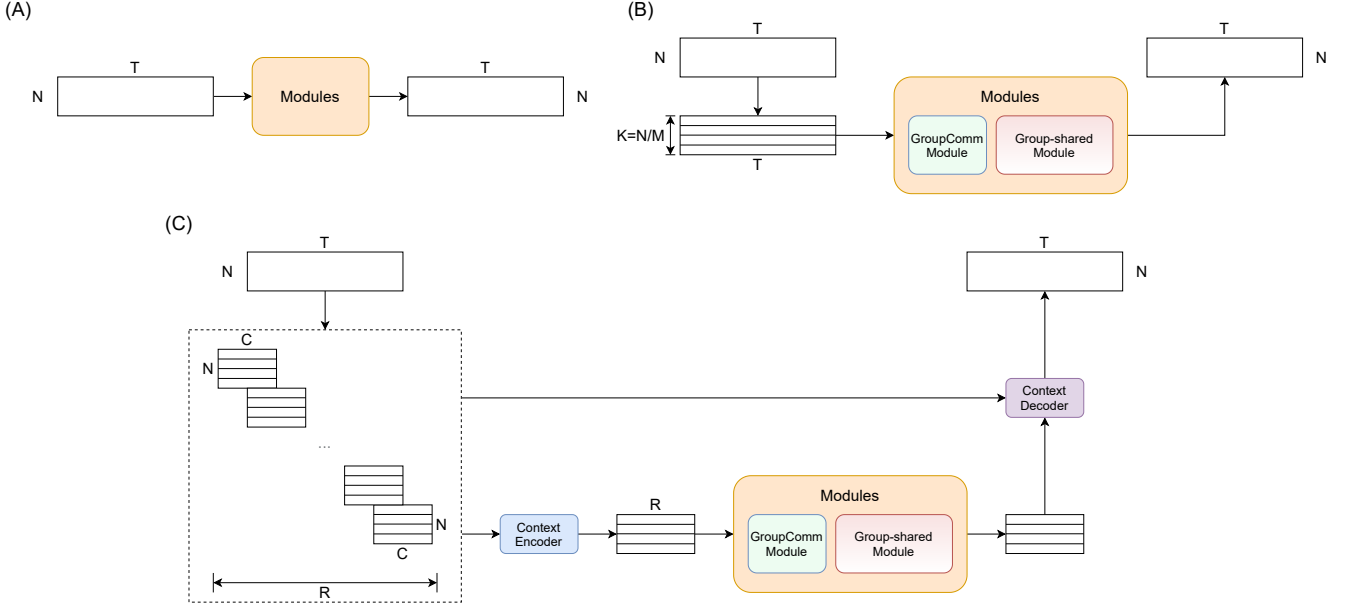


Fig. 1. Flowcharts for (A) standard sequence processing pipeline with a large sequence modeling module; (B) GroupComm-based pipeline, where the features are split into groups with a GroupComm module for inter-group communication. A smaller module for sequence modeling is then shared by all groups; (C) GC3-based pipeline, where the sequence is first segmented into local context frames, and each context is encoded into a single feature. The sequence of summarized features is passed to a GroupComm-based module in (B). The transformed summarized features and the original local context frames are passed to a context decoding module and an overlap-add operation to generate the output with the same size as the input sequence.

for the GC3-based pipeline. Similarly, a GroupComm module is added before each layer in the context codec.

Note that there is no guarantee that the context encoding and decoding modules are reconstructing the original input features as a “codec” typically does, and here, we borrow the name of codec simply to represent the encoding and decoding properties of the two modules.

### C. Network architectures for GroupComm

The original GroupComm module proposed in [38] applied a simple bidirectional LSTM (BLSTM) layer. However, the sequential order of groups may not be important for GroupComm, and the use of recurrent layers may limit the ability for parallelization between groups. Here we investigate two other network architecture options for the GroupComm module.

1) *Transform-average-concatenate*: The transform-average-concatenate (TAC) module was proposed for the multichannel speech separation task with ad-hoc microphone arrays [48]. TAC is similar to the squeeze-and-excitation design paradigm [49] where a global-averaged feature is generated to summarize a pool of features, and the averaged feature is applied back to all the features to form the final outputs with the same dimension.

For the group of features  $\{\mathbf{g}^i\}_{i=1}^K$ , a fully-connected (FC) layer with parametric rectified linear unit (PReLU) activation [50] is applied for the transformation step:

$$\mathbf{f}^i = P(\mathbf{g}^i) \quad (2)$$

where  $P(\cdot)$  is the mapping function defined by the first FC layer and  $\mathbf{f}^i \in \mathbb{R}^D$  denotes the output for group  $i$ . All  $\mathbf{f}^i$  are

then averaged and passed to the second FC layer with PReLU activation for the averaging step:

$$\hat{\mathbf{f}} = R\left(\frac{1}{K} \sum_{i=1}^K \mathbf{f}^i\right) \quad (3)$$

where  $R(\cdot)$  is the mapping function defined by the second FC layer and  $\hat{\mathbf{f}} \in \mathbb{R}^D$  is the output for this step.  $\hat{\mathbf{f}}$  is finally concatenated with the output of the transformation step,  $\mathbf{f}^i$ , and passed to a third FC layer with PReLU activation to generate the final output  $\hat{\mathbf{g}}^i$ :

$$\hat{\mathbf{g}}^i = S([\mathbf{f}^i; \hat{\mathbf{f}}]) \quad (4)$$

where  $S(\cdot)$  is the mapping function defined by the third FC layer and  $[\mathbf{x}; \mathbf{y}]$  denotes the concatenation operation of vectors  $\mathbf{x}$  and  $\mathbf{y}$ . A residual connection is finally added between the module input  $\mathbf{g}^i$  and output  $\hat{\mathbf{g}}^i$ .

TAC does not include any recurrent connections and the processing in the transformation step and concatenation step can be easily run in parallel for all groups. With the same model size, the number of MAC operations and the processing speed of TAC can be fewer and faster than those of a standard BLSTM layer.

2) *Self-attention*: Self-attention (SA) is widely used in various sequence modeling tasks and has already proven its effectiveness in multiple speech-related problems [51]–[55]. SA allows an explicit nonlocal operation between each pair of group features. Following the standard definition of SA, we rewrite the concatenation of group features  $\{\mathbf{g}^i\}_{i=1}^K$  as a matrix  $\mathbf{G} \in \mathbb{R}^{K \times M}$  and apply a multi-head self-attention (MHSAs)

layer:

$$\mathbf{H}_n = \text{Softmax}\left(\frac{\mathbf{Q}_n \mathbf{K}_n^T}{\sqrt{d_k}}\right) \mathbf{V}_n \quad (5)$$

$$\mathbf{G}'_n = [\mathbf{H}_1; \dots; \mathbf{H}_n] \mathbf{W}^o \quad (6)$$

where  $n$  is the number of attention heads,  $\mathbf{W}_n^q, \mathbf{W}_n^k, \mathbf{V}_n^v \in \mathbb{R}^{M \times d_k}$  are the linear transformation matrices for head  $n$ ,  $\mathbf{Q}_n = \mathbf{G} \mathbf{W}_n^q$ ,  $\mathbf{K}_n = \mathbf{G} \mathbf{W}_n^k$ , and  $\mathbf{V}_n = \mathbf{G} \mathbf{W}_n^v$  are the linear transformations for query, key and value, respectively,  $\mathbf{H}_n \in \mathbb{R}^{K \times d_k}$  is the output at head  $n$ , and  $\mathbf{W}^o$  is the linear transformation matrix for the output. Both the concatenation operation and the Softmax nonlinearity are applied across the attention heads.  $\mathbf{G}'$  is then passed to an FC layer with PReLU activation for further transformation, and another FC layer is followed to generate the final output with the same shape as input  $\mathbf{G}'' \in \mathbb{R}^{K \times M}$ .

#### D. Discussions

Splitting a high-dimensional feature into low-dimensional sub-features has also been investigated in architectures for computer vision tasks [56]–[58]. GroupComm shares the same principle as those designs for exploring the nonlinear dependencies at the sub-feature level. However, those designs always concatenate the group-level sub-features back to a high-dimensional feature as the input of an upcoming module, while GroupComm assumes that a small, group-shared module is adequate to preserve the model capacity given the inter-group modeling step. The application of GroupComm in other tasks beyond speech separation is an interesting topic to study.

As discussed in [38], the number of hidden units in both the GroupComm module and the group-shared module in Figure 1 depends on the group size  $K$ . Empirically, we linearly decrease the number of hidden units as  $K$  increases. Assume that for a standard sequence modeling module in Figure 1 (A) with  $N$ -dimensional input features, the number of hidden units or the width of the sequence modeling module is denoted by  $Q$  and both  $N$  and  $Q$  are multiples of  $K$ . Then for a GroupComm-based pipeline, the input dimension for both the GroupComm module and the smaller sequence modeling module becomes  $M = N/K$ , and the model width for the sequence modeling module becomes  $Q/K$ . [38] already conducted experiments on the effect of hyperparameters on the overall model performance and MAC operations, and it was observed that to achieve on par performance with the baseline, a smaller  $K$  requires a deeper sequence modeling module. We show in Section IV that the GC3-based pipeline requires a slightly deeper sequence modeling module due to the existence of the context codec modules; however, the total number of MAC operations is fewer due to the shorter sequence length  $R$  after context encoding.

Context information is widely used as auxiliary information to assist the modeling of a center frame in a sequential input. While many existing studies use a plain concatenation of context features [2], [59]–[61], context codec modules have also been investigated in various studies to learn a nonlinear compact representation [62]–[66]. Specifically, [67] applied a context codec for the multichannel separation task to learn a

set of context-aware filters; however, the context codec did not decrease the sequence length  $T$  but was only used to capture context-aware information. The computational cost in [67] is thus even higher than that without context codec. The main role of the context codec in the GC3 framework is to decrease the computational cost in the actual sequence modeling module by decreasing the sequence length. Moreover, the context codec can also bypass the potential problems of using longer waveform encoder kernels discussed in Section I.

### III. EXPERIMENT CONFIGURATIONS

#### A. Data simulation

We use the same dataset proposed in [48] for the single-channel noisy reverberant speech separation task. The simulated dataset contains 20000, 5000 and 3000 4-second long utterances for training, validation and test sets, respectively. For each utterance, two speech signals and one noise signal are randomly selected from the 100-hour LibriSpeech subset [68] and the 100 Nonspeech Corpus [69], respectively. The overlap ratio between the two speakers is uniformly sampled between 0% and 100%, and the two speech signals are shifted accordingly and rescaled to a random relative SNR between 0 and 5 dB. The relative SNR between the power of the sum of the two clean speech signals and the noise is randomly sampled between 10 and 20 dB. The transformed signals are then convolved with the room impulse responses simulated by the image method [70] using the gpuRIR toolbox [71]. The length and width of all the rooms are randomly sampled between 3 and 10 meters, and the height is randomly sampled between 2.5 and 4 meters. The reverberation time (T60) is randomly sampled between 0.1 and 0.5 seconds. After convolution, the echoic signals are summed to create the mixture for each microphone. The data simulation scripts are publicly available online<sup>1</sup>.

#### B. Backbone model configurations

We use the DPRNN-TasNet architecture [25] as the backbone model for our experiments. A DPRNN segments a sequence of features into overlapping blocks and iteratively applies an intra-block BLSTM layer and an inter-block BLSTM layer to capture the local and global dependencies, respectively. DPRNN-TasNet serves as a strong baseline with a relatively small model size compared with other state-of-the-art network architectures. We use a 2 ms window size (filter length) in the 1-D convolutional waveform encoder and decoder for all experiments, and use ReLU nonlinearity as the activation function for the mask estimation layer. For GroupComm-based and GC3-based models, a GroupComm module is added before each DPRNN block, and the width of the BLSTM layers in the DPRNN blocks is modified according to the number of groups  $K$ . The mask estimation layer in GroupComm-based and GC3-based models is shared by all the groups.

We use stacked GroupComm-BLSTM layers for the context codec modules. A GroupComm-BLSTM layer contains a GroupComm module followed by a residual BLSTM layer.

<sup>1</sup><https://github.com/yluo42/TAC>

A layer normalization (LayerNorm) operation [72] is applied on the BLSTM output followed by a linear projection layer to reshape the output dimension back to the same as the input of the BLSTM at each group. A residual connection is added between the input and output of the BLSTM layer. This configuration is identical to the BLSTM layers used in the DPRNN blocks. The number of groups is also set to be the same as that in the DPRNN blocks. The notations for the hyperparameters can be found in Table I. The model selection for GroupComm modules as well as the application of GroupComm and GC3 in other types of sequence modeling networks is introduced in Section IV-B and Section IV-D, respectively. The implementation of all models is available online<sup>2</sup>.

TABLE I. HYPERPARAMETERS AND THEIR NOTATIONS.

Hyperparameter	Notation
Number of groups	$K$
Group size	$M$
Number of encoder filters	$N$
LSTM input / hidden dimensions	$H_i/H_o$
Number of DPRNN blocks	$L_s$
Number of context codec layers	$L_c$
Context size (in frames)	$C$
DPRNN block size (in frames)	$B$

### C. Evaluation metrics

We report the SI-SDR score [73] for the evaluation of the separation performance, and we report the model size and the number of MAC operations (MACs) as metrics for model complexity. MACs for all models are calculated by an open-source toolbox<sup>3</sup>.

## IV. RESULTS AND ANALYSIS

### A. Experimental results on GroupComm-DPRNN and GC3-DPRNN

We first present the experimental results on the baseline DPRNN, GroupComm-DPRNN and GC3-DPRNN models. Table II lists the separation performance and the corresponding model size and complexity for the three types of models. We first notice that when  $K$  is small (e.g.  $K \leq 4$ ), the GroupComm-DPRNN models can achieve higher performance than plain DPRNN with smaller model size at the cost of an on par or higher model complexity. This is due to the extra MAC operations introduced by the GroupComm module. A larger  $K$  leads to fewer MAC operations; however, the depth of the model has to be modified accordingly to maintain the performance. We explore different hyperparameter settings such that for each  $K$  we obtain a model with less than 5% relative performance degradation. Among all the GroupComm-DPRNN models, we find that the model with  $K = 16$ ,  $N = 128$  and  $L_s = 6$  achieves on par performance as the standard DPRNN model with 2.8% model size and 43.4% MAC operations, and the model with  $K = 32$ ,  $N = 128$

and  $L_s = 10$  only has 5% performance degradation with 1.4% model size and 41.2% MAC operations. These models show that GroupComm is effective in decreasing both the model size and complexity without sacrificing the performance. Moreover, we also conduct experiments on the effect of model width in terms of  $N$  and  $H_i/H_o$  and observe that increasing model width can significantly improve the performance with a much shallower architecture; however, the model complexity can be relatively high. For example, a performance improvement of 0.7 dB can be achieved by  $K = 16$ ,  $N = 256$  and  $L_s = 4$ , while its number of MAC operations is even higher than the baseline DPRNN. This indicates that when the computational cost is not a bottleneck, GroupComm can also be applied to improve the overall performance.

For the GC3-based models, we first investigate the balance between model complexity and performance with different context sizes  $C$ . A larger  $C$  leads to fewer frames for the sequence modeling module, and a smaller DPRNN block size  $B$  can be applied to save model complexity. We observe that models with  $C = 32, 16$  and  $8$  have almost the same performance while differing greatly in complexity; hence, we choose  $C = 32$  for all other experiments. For  $K = 8$ , we see that increasing the number of context codec layers can improve the separation performance, implying that a strong context codec is important. The on par performance can be achieved by  $K = 16$ ,  $N = 128$ ,  $L_s = 8$  and  $L_c = 2$  with a 4.7% model size and 24.4% MAC operations, which saves 19% more MAC operations compared with the GroupComm-only model. The GC3-based model with 5% performance degradation has the configuration of  $K = 32$ ,  $N = 128$ ,  $L_s = 14$  and  $L_c = 2$ , which saves 25% more MAC operations than the GroupComm-only model. Such results prove that GC3-based models are more effective than GroupComm-only models thanks to the context compression operation. Similarly, increasing the model width can also lead to better overall performance with a shallower architecture at the cost of complexity, and in such configurations it is empirically better to keep the depth of the context codec according to the results for  $K = 16$ .

### B. Effect of model architectures for GroupComm

We then evaluate the effect of model architectures for GroupComm. We compare BLSTM with the two other models introduced in Section II-C. For the TAC architecture, the hidden dimension  $D$  is set to  $3H_o$ . For the self-attention (SA) architecture, we use four attention heads with the hidden dimension  $d_k$  set to  $M$ . Such configurations are applied to match the overall model sizes with a BLSTM layer. We use the hyperparameter configurations of the two GC3-based models marked in bold in Table II with  $K = 16$  and  $32$ , respectively. Table III shows the comparison of the three architectures. We find that although SA achieves on par performance as BLSTM in both configurations, TAC obtains even better performance with the fewest MAC operations. Since the number of MAC operations in TAC is fewer than those in both BLSTM and SA and the transformation and concatenation steps in TAC can be run in parallel across groups, we use TAC as the default module for GroupComm in all remaining experiments.

<sup>2</sup><https://github.com/yluo42/GC3>

<sup>3</sup><https://github.com/Lyken17/pytorch-OpCounter>

TABLE II. COMPARISON OF DPRNN, GROUPCOMM-DPRNN AND GC3-DPRNN TASNET MODELS WITH DIFFERENT HYPERPARAMETER CONFIGURATIONS. MACS ARE CALCULATED ON 4-SECOND MIXTURES.

Model	$K$	$M$	$N$	$H_i / H_o$	$L_s$	$L_c$	$C$	$B$	SI-SDR (dB)	Model size	MACs
DPRNN	1	128	128	64 / 128	6	—	—	100	9.0	2.6M	22.1G
GroupComm-DPRNN	2	64	128	64 / 128	4	16	—	100	9.5	2.6M (99.4%)	43.4G (196.4%)
	4	32	128	32 / 64	4				9.4	663.0K (25.3%)	22.4G (101.4%)
	8	16	128	16 / 32	4				8.9	175.5K (6.7%)	11.9G (53.8%)
	8	128	8 / 16	4	6				8.1	51.9K (2.0%)	6.6G (29.9%)
	16	256	16 / 32	2	4				<b>8.9</b>	<b>73.5K (2.8%)</b>	<b>9.6G (43.4%)</b>
	32	4	128	4 / 8	6	—	—	100	8.1	100.7K (3.8%)	12.4G (56.1%)
		8	256	8 / 16	10				9.7	183.9K (7.0%)	23.7G (107.2%)
		8	256	8 / 16	2	—	—	—	7.6	26.0K (1.0%)	5.7G (25.8%)
	32	4	128	4 / 8	10	—	—	—	<b>8.5</b>	<b>37.6K (1.4%)</b>	<b>9.1G (41.2%)</b>
		8	256	8 / 16	4	—	—	—	7.9	38.7K (1.5%)	7.2G (32.6%)
		8	256	8 / 16	4	—	—	—	8.6	60.3K (2.3%)	13.2G (59.7%)
GC3-DPRNN	4	32	128	32 / 64	4	1	32	24	8.9	881.5K (33.7%)	9.2G (41.6%)
		16	128	16 / 32	6		16	32	8.8		10.6G (48.0%)
		8	128	16 / 32	6		8	50	8.8		13.3G (60.2%)
		16	256	8 / 16	8		4	64	9.3		18.6G (84.2%)
	8	16	128	16 / 32	6	1	32	24	8.7	314.4K (12.0%)	5.4G (24.4%)
		16	256	16 / 32	6	2			9.3	369.9K (14.1%)	8.1G (36.7%)
		16	256	16 / 32	6	1			<b>8.9</b>	<b>124.1K (4.7%)</b>	<b>5.4G (24.4%)</b>
	32	4	128	4 / 8	14	2	32	24	9.0	322.9K (12.3%)	10.9G (49.3%)
		8	256	8 / 16	8	2			<b>8.3</b>	<b>57.1K (2.2%)</b>	<b>3.6G (16.3%)</b>
		8	256	8 / 16	8	2			9.2	132.6K (5.1%)	10.7G (48.4%)

TABLE III. COMPARISON OF GC3-DPRNN MODELS WITH DIFFERENT MODEL ARCHITECTURES FOR GROUPCOMM.

GroupComm module	$K$	SI-SDR (dB)	Model size	MACs
BLSTM	16	8.9	124.1K	5.4G (24.4%)
	32	8.3	57.1K	3.6G (16.3%)
TAC	16	<b>9.1</b>	<b>123.8K</b>	<b>3.9G (17.6%)</b>
	32	<b>8.6</b>	<b>56.3K</b>	<b>2.6G (11.8%)</b>
SA	16	8.9	123.7K	4.5G (20.3%)
	32	8.2	56.5K	3.0G (13.4%)

### C. Effect of overlap ratio across groups

The default group segmentation configuration in all experiments above assumes no overlap between groups. However, a 50% overlap is always applied in sequence segmentation operations such as context segmentation in the context codec and block segmentation in DPRNN modules. It is thus interesting to see whether adding overlap between groups can improve the performance. Table IV provides the separation performance as well as the model size and complexity for different overlap ratios between groups. We observe that adding a 25% percent overlap between groups increases the number of MAC operations while not leading to an better performance, but a 50% overlap between groups can improve the overall performance. Compared with the model in Table II with a similar performance ( $K = 8$ ,  $N = 128$ ,  $L_c = 2$ ), such a model has a smaller model size and fewer MAC operations. This shows that compared with using a smaller number of groups  $K$ , adding proper overlap between groups is a more effective method for improving the performance.

### D. Application of GC3 in other types of architectures

There are also various other lightweight model architectures beyond DPRNN that have been proposed in recent years. Here we investigate the effectiveness of GC3 in three other types of architectures:

TABLE IV. EFFECT OF GROUP OVERLAP RATIO ON MODEL COMPLEXITY AND SEPARATION PERFORMANCE IN GC3-DPRNN MODELS.

Group overlap	SI-SDR (dB)	Model size	MACs
0%	9.1	123.8K	3.9G (17.6%)
25%	9.0		4.9G (22.0%)
50%	9.4		6.9G (31.3%)

- 1) *Conv-TasNet* [14]: Conv-TasNet applied a temporal convolutional network (TCN) as the sequence modeling module to perform time-domain speech separation. Each TCN block contained a depthwise-separable convolution layer [74] with PReLU nonlinearity and a LayerNorm operation, where the convolution layer contains an exponentially increased dilation factor to increase the overall receptive field of the TCN. Here, we apply 2 TCNs with 6 convolutional blocks in each TCN to achieve the same level of model size as the DPRNN-TasNet. We use the same number of TCN layers and convolutional blocks for the GC3-equipped modification.
- 2) *Sudo rm -rf* [18]: Sudo rm -rf proposed a U-net style convolutional block where multiple levels of downsampling and upsampling layers were applied to extract features at different scales. Each downsampling layer contained a depthwise separation convolution operation similar to Conv-TasNet, and each upsampling layer contained a bilinear interpolation operation. We use the default configuration, which contains 5 downsampling and upsampling layers in each U-net block, and we use 8 blocks for both baseline and GC3-equipped modification.
- 3) *Dual-path Transformer (DPTNet)* [27]: DPTNet replaced the BLSTM layers in DPRNN with modified Transformer layers [51], where the fully connected layer in the default transformer encoder layer [51] was

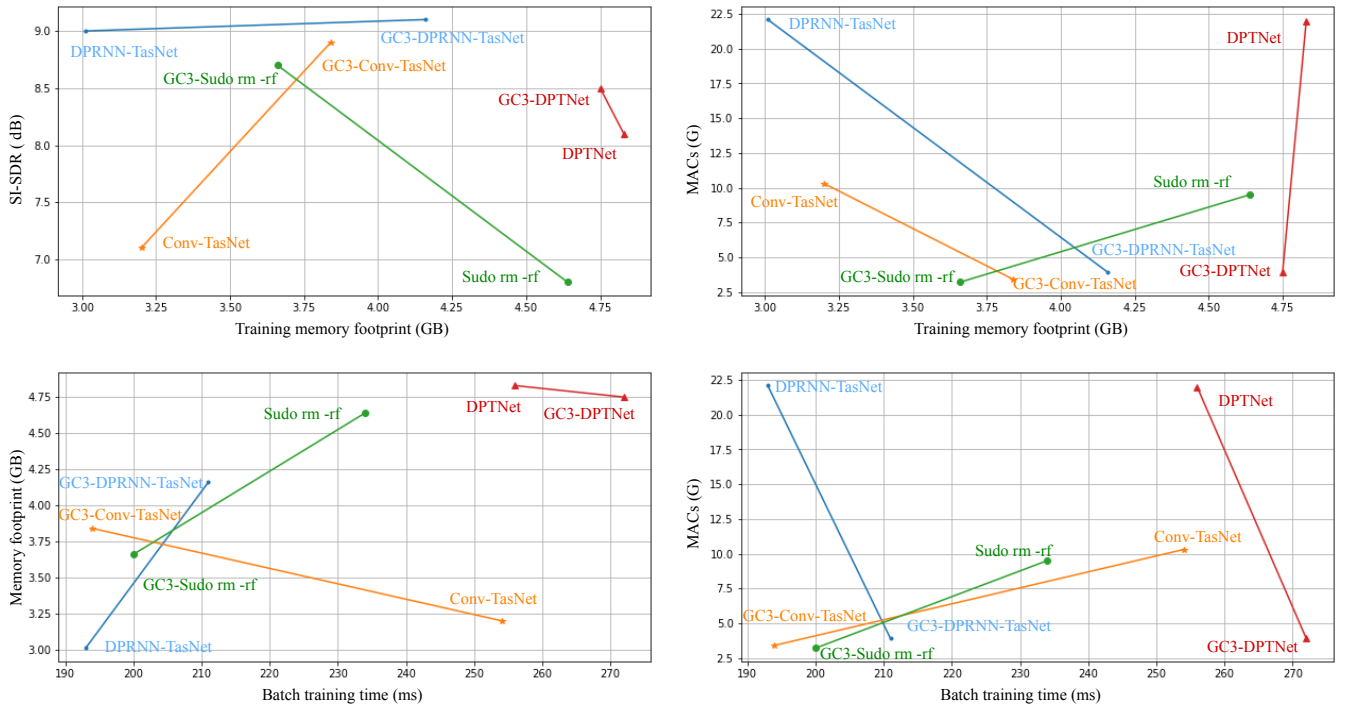


Fig. 2. Training phase statistics for the four architectures. The training memory footprint, batch-level training time, SI-SDR performance, and number of MAC operations are visualized.

replaced by an LSTM layer to learn the positional information in the sequence. We use the default configuration that contains 6 Transformer layers, and for GC3-equipped DPTNet we use 8 Transformer layers similar to our configuration for GC3-DPRNN. The learning rate warm-up configuration is also set the same as the recommended configuration, where the first 4000 iterations are used for the warm-up stage.

We encourage the readers to refer to the corresponding literature for details about the three models. The same 2-layer GroupComm-based context encoder and decoder are applied in all GC3-equipped models, and all other configurations, including the window size in the waveform encoder/decoder, the use of ReLU nonlinearity for mask estimation, and the number of encoder filters  $N$ , remain unchanged.

Table V presents the performance of the three architectures with their GC3-equipped modifications. For CNN-based models such as Conv-TasNet and Sudo rm -rf, GC3-equipped modifications achieve significantly better performance with as small as 2.5% model size and as few as 33.0% MAC operations. Since CNN-based models have a fixed receptive field and it has been investigated that a long receptive field is important for such sequence modeling tasks [14], a small CNN-based network may fail to achieve satisfactory performance due to its small receptive field. The context codec squeezes the long sequence by a factor of  $C/2$  and makes the receptive fields of such small models adequate to cover longer sequential context, thus significantly improving the performance. For the transformer-based DPTNet model, the baseline performance is

TABLE V. COMPARISON OF CONV-TASNET, SUDO RM -RF, AND DPTNET ARCHITECTURES WITH AND WITHOUT GC3.

Model	SI-SDR (dB)	Model size	MACs
Conv-TasNet [14] + GC3	7.1 <b>8.9</b>	2.5M <b>191.2K (7.6%)</b>	10.3G <b>3.4G (33.0%)</b>
Sudo rm -rf [18] + GC3	6.8 <b>8.7</b>	2.4M <b>60.0K (2.5%)</b>	9.5G <b>3.2G (33.7%)</b>
DPTNet [27] + GC3	8.1 <b>8.5</b>	2.8M <b>128.6K (4.6%)</b>	21.8G <b>3.9G (17.9%)</b>

worse than that of the baseline DPRNN. One possible reason is the noisy reverberant property of our simulated dataset, but an in-depth analysis of the performance of such transformer-based systems on the noisy reverberant separation task is beyond the scope of this paper. Nevertheless, adding the GC3 design to DPTNet improves the performance and significantly decreases the number of MAC operations, proving that GC3 can be easily deployed into other types of sequence modeling networks beyond recurrent networks.

#### E. Training phase statistics for different models

Beyond the model size and number of MAC operations, the memory footprint and training speed are also important indicators for model complexity, as small models can also be slow to train and require enormous memory. To compare such training phase statistics of different models, Figure 2 visualizes the relationship between the training memory footprint, batch-level training time, SI-SDR performance and the number of MAC operations. The memory footprint and training time are

evaluated with a batch size of 4. For DPRNN-TasNet and Conv-TasNet, GC3 increases the training memory footprint by a relatively large margin; however, the training time is only slightly increased. For Sudo rm -rf, GC3 not only requires less memory but also makes the training 15% faster. For DPTNet, memory consumption is slightly lower while the training speed is slightly slower. In general, GC3 does not increase the training speed of the model, and for certain architectures, GC3 may slightly increase the training phase memory consumption.

## V. CONCLUSION AND FUTURE WORKS

In this paper, we proposed **Group Communication with Context Codec (GC3)**, a simple plug-and-play module for significantly decreasing both the model size and complexity while maintaining model performance. The group communication (GroupComm) module in GC3 splits a high-dimensional feature into groups of low-dimensional features and applies a module to capture the inter-group dependency. Instead of concatenating the low-dimensional features back to a high-dimensional feature for further processing, a model with a significantly smaller width is shared by all groups and run in parallel. A context codec is applied to decrease the length of a sequential feature and thus decrease the complexity of the sequence modeling module. A context encoder compresses the temporal context of local features into a single feature, and a context decoder decompresses the transformed feature back to the context features. We conducted experiments on four different types of sequence modeling architectures and showed that GC3 can achieve on par or better performance than the baseline, proving that GC3 is a universal module for changing any model into an ultra-lightweight counterpart. We also explored the model design and hyperparameters for GC3 on their effects on the model size, complexity and performance.

Note that we did not consider the application of model binarization or quantization techniques together with GC3 in this paper. Such techniques can significantly decrease the model storage size and MAC operations without changing the model architecture, although they typically lead to certain levels of performance degradation [75]. Applying GC3 together with such techniques may require an increase in the overall model size to achieve on par performance, and the actual model configuration may be directly related to the target platform to which the model will be deployed. Moreover, the GroupComm module can be used as a prototype module in any neural architecture search (NAS) algorithm [76] to search for better both model architecture and layer organization, balancing the model size, complexity and performance. We leave such directions as future works.

## VI. ACKNOWLEDGMENTS

This work was funded by a grant from the National Institute of Health, NIDCD, DC014279; and a National Science Foundation CAREER Award.

## REFERENCES

- [1] P.-S. Huang, M. Kim, M. Hasegawa-Johnson, and P. Smaragdis, “Deep learning for monaural speech separation,” in *Acoustics, Speech and Signal Processing (ICASSP), 2014 IEEE International Conference on*. IEEE, 2014, pp. 1562–1566.
- [2] D. Yu, M. Kolbæk, Z.-H. Tan, and J. Jensen, “Permutation invariant training of deep models for speaker-independent multi-talker speech separation,” in *Acoustics, Speech and Signal Processing (ICASSP), 2017 IEEE International Conference on*. IEEE, 2017, pp. 241–245.
- [3] M. Kolbæk, D. Yu, Z.-H. Tan, and J. Jensen, “Multitalker speech separation with utterance-level permutation invariant training of deep recurrent neural networks,” *IEEE/ACM Transactions on Audio, Speech, and Language Processing (TASLP)*, vol. 25, no. 10, pp. 1901–1913, 2017.
- [4] Y. Isik, J. Le Roux, Z. Chen, S. Watanabe, and J. R. Hershey, “Single-channel multi-speaker separation using deep clustering,” *Proc. Interspeech*, pp. 545–549, 2016.
- [5] Y. Luo, Z. Chen, and N. Mesgarani, “Speaker-independent speech separation with deep attractor network,” *IEEE/ACM Transactions on Audio, Speech, and Language Processing (TASLP)*, vol. 26, no. 4, pp. 787–796, 2018. [Online]. Available: <http://dx.doi.org/10.1109/TASLP.2018.2795749>
- [6] P. Chandna, M. Miron, J. Janer, and E. Gómez, “Monoaural audio source separation using deep convolutional neural networks,” in *International conference on latent variable analysis and signal separation*. Springer, 2017, pp. 258–266.
- [7] A. Jansson, E. Humphrey, N. Montecchio, R. Bittner, A. Kumar, and T. Weyde, “Singing voice separation with deep u-net convolutional networks,” in *ISMIR*, 2017, pp. 745–751.
- [8] N. Takahashi and Y. Mitsuishi, “Multi-scale multi-band densenets for audio source separation,” in *2017 IEEE Workshop on Applications of Signal Processing to Audio and Acoustics (WASPAA)*. IEEE, 2017, pp. 21–25.
- [9] S. Park, T. Kim, K. Lee, and N. Kwak, “Music source separation using stacked hourglass networks.” in *ISMIR*, 2018, pp. 289–296.
- [10] D. Yin, C. Luo, Z. Xiong, and W. Zeng, “PHASEN: A phase-and-harmonics-aware speech enhancement network.” in *AAAI*, 2020, pp. 9458–9465.
- [11] N. Takahashi and Y. Mitsuishi, “D3net: Densely connected multililated densenet for music source separation,” *arXiv preprint arXiv:2010.01733*, 2020.
- [12] D. Stoller, S. Ewert, and S. Dixon, “Wave-U-Net: A multi-scale neural network for end-to-end audio source separation.” in *ISMIR*, 2018, pp. 334–340.
- [13] S. Venkataramani, J. Casebeer, and P. Smaragdis, “End-to-end source separation with adaptive front-ends,” in *2018 52nd Asilomar Conference on Signals, Systems, and Computers*. IEEE, 2018, pp. 684–688.
- [14] Y. Luo and N. Mesgarani, “Conv-TasNet: Surpassing ideal time-frequency magnitude masking for speech separation,” *IEEE/ACM Transactions on Audio, Speech, and Language Processing (TASLP)*, vol. 27, no. 8, pp. 1256–1266, 2019.
- [15] F. Lluís, J. Pons, and X. Serra, “End-to-end music source separation: Is it possible in the waveform domain?” *Proc. Interspeech*, pp. 4619–4623, 2019.
- [16] A. Pandey and D. Wang, “A new framework for cnn-based speech enhancement in the time domain,” *IEEE/ACM Transactions on Audio, Speech, and Language Processing (TASLP)*, vol. 27, no. 7, pp. 1179–1188, 2019.
- [17] L. Zhang, Z. Shi, J. Han, A. Shi, and D. Ma, “Furcanext: End-to-end monaural speech separation with dynamic gated dilated temporal convolutional networks,” in *International Conference on Multimedia Modeling*. Springer, 2020, pp. 653–665.
- [18] E. Tzinis, Z. Wang, and P. Smaragdis, “Sudo rm-rf: Efficient networks for universal audio source separation,” in *2020 IEEE 30th International Workshop on Machine Learning for Signal Processing (MLSP)*. IEEE, 2020, pp. 1–6.
- [19] L. Sun, J. Du, L.-R. Dai, and C.-H. Lee, “Multiple-target deep learning for LSTM-RNN based speech enhancement,” in *2017 Hands-free Speech Communications and Microphone Arrays (HSCMA)*. IEEE, 2017, pp. 136–140.

- [20] G. Naithani, T. Barker, G. Parascandolo, L. Bramsl, N. H. Pontoppidan, T. Virtanen *et al.*, “Low latency sound source separation using convolutional recurrent neural networks,” in *2017 IEEE Workshop on Applications of Signal Processing to Audio and Acoustics (WASPAA)*. IEEE, 2017, pp. 71–75.
- [21] H. Zhao, S. Zarar, I. Tashev, and C.-H. Lee, “Convolutional-recurrent neural networks for speech enhancement,” in *Acoustics, Speech and Signal Processing (ICASSP), 2018 IEEE International Conference on*. IEEE, 2018, pp. 2401–2405.
- [22] N. Takahashi, N. Goswami, and Y. Mitsufuji, “MMDenseLSTM: An efficient combination of convolutional and recurrent neural networks for audio source separation,” in *2018 16th International Workshop on Acoustic Signal Enhancement (IWAENC)*. IEEE, 2018, pp. 106–110.
- [23] K. Tan and D. Wang, “A convolutional recurrent neural network for real-time speech enhancement.” in *Proc. Interspeech*, 2018, pp. 3229–3233.
- [24] Y. Hu, Y. Liu, S. Lv, M. Xing, S. Zhang, Y. Fu, J. Wu, B. Zhang, and L. Xie, “DCCRN: Deep complex convolution recurrent network for phase-aware speech enhancement,” *arXiv preprint arXiv:2008.00264*, 2020.
- [25] Y. Luo, Z. Chen, and T. Yoshioka, “Dual-path RNN: efficient long sequence modeling for time-domain single-channel speech separation,” in *Acoustics, Speech and Signal Processing (ICASSP), 2020 IEEE International Conference on*. IEEE, 2020, pp. 46–50.
- [26] E. Nachmani, Y. Adi, and L. Wolf, “Voice separation with an unknown number of multiple speakers,” *arXiv preprint arXiv:2003.01531*, 2020.
- [27] J. Chen, Q. Mao, and D. Liu, “Dual-path transformer network: Direct context-aware modeling for end-to-end monaural speech separation,” *Proc. Interspeech*, pp. 2642–2646, 2020.
- [28] K. Kinoshita, T. von Neumann, M. Delcroix, T. Nakatani, and R. Haeb-Umbach, “Multi-path RNN for hierarchical modeling of long sequential data and its application to speaker stream separation,” *Proc. Interspeech 2020*, pp. 2652–2656, 2020.
- [29] K. Tan, B. Xu, A. Kumar, E. Nachmani, and Y. Adi, “SAGRNN: Self-attentive gated rnn for binaural speaker separation with interaural cue preservation,” *arXiv preprint arXiv:2009.01381*, 2020.
- [30] H. Mazzawi, X. Gonzalvo, A. Kracun, P. Sridhar, N. Subrahmanya, I. Lopez-Moreno, H.-J. Park, and P. Violette, “Improving keyword spotting and language identification via neural architecture search at scale.” in *Proc. Interspeech*, 2019, pp. 1278–1282.
- [31] S. Hu, X. Xie, S. Liu, M. Geng, X. Liu, and H. Meng, “Neural architecture search for speech recognition,” *arXiv preprint arXiv:2007.08818*, 2020.
- [32] R. Aihara, T. Hanazawa, Y. Okato, G. Wichern, and J. Le Roux, “Teacher-student deep clustering for low-delay single channel speech separation,” in *Acoustics, Speech and Signal Processing (ICASSP), 2019 IEEE International Conference on*. IEEE, 2019, pp. 690–694.
- [33] M. Kim and P. Smaragdis, “Bitwise neural networks for efficient single-channel source separation,” in *Acoustics, Speech and Signal Processing (ICASSP), 2018 IEEE International Conference on*. IEEE, 2018, pp. 701–705.
- [34] S. Kim, M. Maity, and M. Kim, “Incremental binarization on recurrent neural networks for single-channel source separation,” in *Acoustics, Speech and Signal Processing (ICASSP), 2019 IEEE International Conference on*. IEEE, 2019, pp. 376–380.
- [35] S. Kim, H. Yang, and M. Kim, “Boosted locality sensitive hashing: Discriminative binary codes for source separation,” in *Acoustics, Speech and Signal Processing (ICASSP), 2020 IEEE International Conference on*. IEEE, 2020, pp. 106–110.
- [36] G. Hinton, O. Vinyals, and J. Dean, “Distilling the knowledge in a neural network,” *arXiv preprint arXiv:1503.02531*, 2015.
- [37] J.-H. Luo, J. Wu, and W. Lin, “Thinet: A filter level pruning method for deep neural network compression,” in *Proceedings of the IEEE international conference on computer vision*, 2017, pp. 5058–5066.
- [38] Y. Luo, C. Han, and N. Mesgarani, “Ultra-lightweight speech separation via group communication,” *arXiv preprint arXiv:2011.08397*, 2020.
- [39] J. Li, A. Mohamed, G. Zweig, and Y. Gong, “LSTM time and frequency recurrence for automatic speech recognition,” in *Automatic Speech Recognition and Understanding (ASRU), 2015 IEEE Workshop on*. IEEE, 2015, pp. 187–191.
- [40] Q. Wang, J. Du, L.-R. Dai, and C.-H. Lee, “Joint noise and mask aware training for DNN-based speech enhancement with sub-band features,” in *2017 Hands-free Speech Communications and Microphone Arrays (HSCMA)*. IEEE, 2017, pp. 101–105.
- [41] X. Zhang and D. Wang, “Deep learning based binaural speech separation in reverberant environments,” *IEEE/ACM Transactions on Audio, Speech, and Language Processing (TASLP)*, vol. 25, no. 5, pp. 1075–1084, 2017.
- [42] X. Li and R. Horaud, “Multichannel speech enhancement based on time-frequency masking using subband long short-term memory,” in *2019 IEEE Workshop on Applications of Signal Processing to Audio and Acoustics (WASPAA)*. IEEE, 2019, pp. 298–302.
- [43] J. Li, A. Mohamed, G. Zweig, and Y. Gong, “Exploring multidimensional LSTMs for large vocabulary ASR,” in *Acoustics, Speech and Signal Processing (ICASSP), 2016 IEEE International Conference on*. IEEE, 2016, pp. 4940–4944.
- [44] T. N. Sainath and B. Li, “Modeling time-frequency patterns with LSTM vs. convolutional architectures for lvcsr tasks,” *Proc. Interspeech*, pp. 813–817, 2016.
- [45] C. Xu, W. Rao, X. Xiao, E. S. Chng, and H. Li, “Single channel speech separation with constrained utterance level permutation invariant training using grid LSTM,” in *Acoustics, Speech and Signal Processing (ICASSP), 2018 IEEE International Conference on*. IEEE, 2018, pp. 6–10.
- [46] N. Whitehead and A. Fit-Florea, “Precision & performance: Floating point and ieee 754 compliance for nvidia gpus,” *rn (A+B)*, vol. 21, no. 1, pp. 18 749–19 424, 2011.
- [47] Y. Luo and N. Mesgarani, “TasNet: time-domain audio separation network for real-time, single-channel speech separation,” in *Acoustics, Speech and Signal Processing (ICASSP), 2018 IEEE International Conference on*. IEEE, 2018.
- [48] Y. Luo, Z. Chen, N. Mesgarani, and T. Yoshioka, “End-to-end microphone permutation and number invariant multi-channel speech separation,” in *Acoustics, Speech and Signal Processing (ICASSP), 2020 IEEE International Conference on*. IEEE, 2020, pp. 6394–6398.
- [49] J. Hu, L. Shen, and G. Sun, “Squeeze-and-excitation networks,” in *Proceedings of the IEEE conference on computer vision and pattern recognition*, 2018, pp. 7132–7141.
- [50] K. He, X. Zhang, S. Ren, and J. Sun, “Delving deep into rectifiers: Surpassing human-level performance on imagenet classification,” in *Proceedings of the IEEE international conference on computer vision*, 2015, pp. 1026–1034.
- [51] A. Vaswani, N. Shazeer, N. Parmar, J. Uszkoreit, L. Jones, A. N. Gomez, L. Kaiser, and I. Polosukhin, “Attention is all you need,” in *Advances in neural information processing systems*, 2017, pp. 5998–6008.
- [52] L. Dong, S. Xu, and B. Xu, “Speech-transformer: a no-recurrence sequence-to-sequence model for speech recognition,” in *Acoustics, Speech and Signal Processing (ICASSP), 2018 IEEE International Conference on*. IEEE, 2018, pp. 5884–5888.
- [53] N. Li, S. Liu, Y. Liu, S. Zhao, and M. Liu, “Neural speech synthesis with transformer network,” in *Proceedings of the AAAI Conference on Artificial Intelligence*, vol. 33, 2019, pp. 6706–6713.
- [54] E. Tsunoo, Y. Kashiwagi, T. Kumakura, and S. Watanabe, “Transformer ASR with contextual block processing,” in *Automatic Speech Recognition and Understanding (ASRU), 2019 IEEE Workshop on*. IEEE, 2019, pp. 427–433.
- [55] S. Karita, N. Chen, T. Hayashi, T. Hori, H. Inaguma, Z. Jiang, M. Someki, N. E. Y. Soplin, R. Yamamoto, X. Wang *et al.*, “A comparative study on transformer vs rnn in speech applications,” in

- Automatic Speech Recognition and Understanding (ASRU), 2019 IEEE Workshop on.* IEEE, 2019, pp. 449–456.
- [56] S. Gao, M.-M. Cheng, K. Zhao, X.-Y. Zhang, M.-H. Yang, and P. H. Torr, “Res2net: A new multi-scale backbone architecture,” *IEEE transactions on pattern analysis and machine intelligence (TPAMI)*, 2019.
- [57] H. Zhang, C. Wu, Z. Zhang, Y. Zhu, Z. Zhang, H. Lin, Y. Sun, T. He, J. Mueller, R. Manmatha *et al.*, “ResNeSt: Split-attention networks,” *arXiv preprint arXiv:2004.08955*, 2020.
- [58] K. Han, Y. Wang, Q. Tian, J. Guo, C. Xu, and C. Xu, “GhostNet: More features from cheap operations,” in *Proceedings of the IEEE/CVF Conference on Computer Vision and Pattern Recognition*, 2020, pp. 1580–1589.
- [59] Y. Xu, J. Du, L.-R. Dai, and C.-H. Lee, “An experimental study on speech enhancement based on deep neural networks,” *IEEE Signal processing letters*, vol. 21, no. 1, pp. 65–68, 2013.
- [60] —, “A regression approach to speech enhancement based on deep neural networks,” *IEEE/ACM Transactions on Audio, Speech, and Language Processing (TASLP)*, vol. 23, no. 1, pp. 7–19, 2014.
- [61] S. Araki, T. Hayashi, M. Delcroix, M. Fujimoto, K. Takeda, and T. Nakatani, “Exploring multi-channel features for denoising-autoencoder-based speech enhancement,” in *Acoustics, Speech and Signal Processing (ICASSP), 2015 IEEE International Conference on*. IEEE, 2015, pp. 116–120.
- [62] T. Mikolov, I. Sutskever, K. Chen, G. S. Corrado, and J. Dean, “Distributed representations of words and phrases and their compositionality,” in *Advances in neural information processing systems*, 2013, pp. 3111–3119.
- [63] X. Chen, X. Qiu, C. Zhu, P. Liu, and X.-J. Huang, “Long short-term memory neural networks for chinese word segmentation,” in *Proceedings of the 2015 Conference on Empirical Methods in Natural Language Processing*, 2015, pp. 1197–1206.
- [64] D. Pathak, P. Krahenbuhl, J. Donahue, T. Darrell, and A. A. Efros, “Context encoders: Feature learning by inpainting,” in *Proceedings of the IEEE conference on computer vision and pattern recognition*, 2016, pp. 2536–2544.
- [65] S. Mehri, K. Kumar, I. Gulrajani, R. Kumar, S. Jain, J. Sotelo, A. Courville, and Y. Bengio, “SampleRNN: An unconditional end-to-end neural audio generation model,” *arXiv preprint arXiv:1612.07837*, 2016.
- [66] A. Marafioti, N. Perraudin, N. Holighaus, and P. Majdak, “A context encoder for audio inpainting,” *IEEE/ACM Transactions on Audio, Speech, and Language Processing (TASLP)*, vol. 27, no. 12, pp. 2362–2372, 2019.
- [67] Y. Luo and N. Mesgarani, “Implicit filter-and-sum network for multi-channel speech separation,” *arXiv preprint arXiv:2011.08401*, 2020.
- [68] V. Panayotov, G. Chen, D. Povey, and S. Khudanpur, “Librispeech: an ASR corpus based on public domain audio books,” in *Acoustics, Speech and Signal Processing (ICASSP), 2015 IEEE International Conference on*. IEEE, 2015, pp. 5206–5210.
- [69] G. Hu, “100 Nonspeech Sounds,” <http://web.cse.ohio-state.edu/pnl/corpus/HuNonspeech/HuCorpus.html>.
- [70] J. B. Allen and D. A. Berkley, “Image method for efficiently simulating small-room acoustics,” *The Journal of the Acoustical Society of America*, vol. 65, no. 4, pp. 943–950, 1979.
- [71] D. Diaz-Guerra, A. Miguel, and J. R. Beltran, “gpuRIR: A python library for room impulse response simulation with gpu acceleration,” *Multimedia Tools and Applications*, pp. 1–19, 2020.
- [72] J. L. Ba, J. R. Kiros, and G. E. Hinton, “Layer normalization,” *arXiv preprint arXiv:1607.06450*, 2016.
- [73] J. Le Roux, S. Wisdom, H. Erdogan, and J. R. Hershey, “SDR–half-baked or well done?” in *Acoustics, Speech and Signal Processing (ICASSP), 2019 IEEE International Conference on*. IEEE, 2019, pp. 626–630.
- [74] F. Chollet, “Xception: Deep learning with depthwise separable convolutions,” *arXiv preprint*, 2016.
- [75] T. Simons and D.-J. Lee, “A review of binarized neural networks,” *Electronics*, vol. 8, no. 6, p. 661, 2019.
- [76] H. Liu, K. Simonyan, and Y. Yang, “DARTS: Differentiable architecture search,” in *International Conference on Learning Representations*, 2018.